Polímeros
ISSN 1678-5169 (Online)

https://doi.org/10.1590/0104-1428.20220018

ORIGINAL ARTICLE

Influence of processing parameters on mechanical and thermal behavior of PLA/PBAT blend[a]

Virnna Cristhielle Santana Barbosa[1]*, Ana Maria Furtado de Sousa[1] and Ana Lúcia Nazareth da Silva[2,3]

[1]Instituto de Química, Universidade do Estado do Rio de Janeiro – UERJ, Rio de Janeiro, RJ, Brasil
[2]Instituto de Macromoléculas Professora Eloisa Mano, Universidade Federal do Rio de Janeiro – UFRJ, Rio de Janeiro, RJ, Brasil
[3]Programa de Engenharia Ambiental, Universidade Federal do Rio de Janeiro – UFRJ, Rio de Janeiro, RJ, Brasil

[a]This paper has been partially presented at the 16th Brazilian Polymer Congress, held on-line, 24-28/Oct/2021.

**ananazareth@ima.ufrj.br*

Abstract

This study evaluates the influence of processing parameters and reactive extrusion on the mechanical and thermal behavior of PLA/PBAT (70/30, wt.%) blends. The effect of reverse mixing elements (RME) and feed rate (FR) of the extruder were studied using a factorial design of experiments. Further, two types of blends were processed by extrusion molding: with (AD) and without (NAD) additives. The FTIR analysis showed that PLA suffered some degree of degradation, being this process more pronounced for NAD blends. A better interaction between the PLA and PBAT phases occurred for reactive extrusion, inducing an improvement in the impact properties and thermal behavior. The cold crystallization temperature of the NAD blends decreased when two RME was used. Both RME and FR parameters affected the elastic modulus of NAD blends, while only FR affected the elastic modulus of AD blends.

Keywords: *poly(lactic acid) (PLA), poly(butylene adipate-co-terephthalate) (PBAT), reactive extrusion.*

How to cite: Barbosa, V. C. S., Sousa, A. M. F., & Silva, A. L. N. (2022). Influence of processing parameters on mechanical and thermal behavior of PLA/PBAT blend. *Polímeros: Ciência e Tecnologia*, *32*(3), e2022033. https://doi.org/10.1590/0104-1428.20220018

1. Introduction

Researches based on polymers from biological sources and/or biodegradable polymeric materials have become one of the most interesting fields of macromolecular science and technology[1]. In this context, poly(lactic acid) (PLA) and poly(butylene adipate-co-terephthalate) (PBAT) are biopolymers from renewable and fossil sources, respectively, which have performance properties comparable to those of traditional thermoplastics. PLA and PBAT appear as favorable alternatives for application in several segments, especially in packaging[2-4]. PLA/PBAT blends attract interest due to the improvements promoted by their combinations of properties, in addition to having a significant commercial potential[5-8]. PLA has certain characteristics that limit its application, such as low toughness at room temperature and low heat deflection temperature compared to conventional polymers. This behavior can be balanced by blending with PBAT, which has a high elongation at break and low elastic modulus, with a mechanical behavior similar to a thermoplastic elastomer, thus being considered an excellent option for combining the characteristics of two polymers[5,9,10].

PLA and PBAT are polymers thermodynamically immiscible, which can compromise their blend morphology and, consequently, their final performance[11]. The control of the complex morphology of the immiscible polymeric blends is an important factor for developing new materials. In this context, it is also important to study the effect of additive incorporation and the processing parameters on the interaction improvement between the phases of immiscible blends[11,12].

Arruda et al.[10] studied the action of multifunctional epoxide as a chain extender, available on the market as Joncryl, on the mechanical behavior of PLA/PBAT blends. They obtained an improvement in thermal stability and an increase in complex viscosity; however, the chain extender was not sufficient to provide greater adhesion between phases[13]. Hongdilokkul et al.[14] used di-(tert.-butyl-peroxy-isopropyl) benzene peroxide, commercially known as Perkadox, as a reactive agent in the PLA/PBAT blend. The results showed improvements in the toughness properties of the blend and in interfacial adhesion. Rigolin et al.[11] also evaluated a method to obtain flexible blends with good interfacial adhesion. For this purpose, PLA was grafted with maleic anhydride, and the resulting PLA-g-MA was used as a matrix with the addition of dicumyl peroxide. The modification generated

low molar mass blends, but with homogeneous dispersed phase morphology compared to the PLA/PBAT.

The extruder has at least three different types of elements that can be changed and configured. The transport elements, to transport the material along the length of the thread profile; mixing elements, to favor the mixing of constituent materials exerting direct influence on shear; and reverse elements, with the aim of extending the residence time and favoring a more intensive mixing[15,16]. Processing characteristics can be induced, from mild to severe, according to the configuration of the screw thread and its elements, changing the extent of physicochemical changes that influence the quality of the product[10,17,18]. The inclusion of reverse elements can widen the residence time distribution, especially at low feed rates[12], in addition to increasing the mixing and dispersion of the material in the extruder, as the geometry of the reverse elements must ensure a more intense shear of the material[19]. Ambrósio et al.[20] studied the effects of extrusion feed rate on the extrusion of a Polybutylene Terephthalate (PBT)/ Acrylonitrile butadiene styrene (ABS) blend. For them, the reduction in the feed rate contributed to the reduction of the Izod impact resistance. For Yeh et al.[21], the increase in the extruder feed rate reduced the average residence time, and this effect was more pronounced than the screw speed.

The novelty of the present work is the study of the influence of processing parameters, such as the screw profile and feed rate, on the mechanical and thermal properties of blends based on PLA and PBAT. The processing was carried out by non-reactive extrusion and reactive extrusion of a PLA/PBAT composition (70/30, wt.%).

2. Materials and Methods

2.1 Materials

The biopolymers PLA Ingeo™ 2003 from NatureWorks LLC (data sheet value of melt flow index: 6 g.10min^{-1} at 2.26kg/210°C, test result value of melt flow index: 6.24 ± 0.54 g.10min^{-1} at 2.26kg/210°C, Mw: 206,239 g/mol, and polydispersity index:1.7) and PBAT Ecoflex® FBX 7011 from BASF (melt flow index: 2.7 – 4.9 g.10min^{-1} at 2.26kg/190°C) were purchased from Oeko Bioplásticos. Maleic anhydride (MA) grade STBH9257 and dicumyl peroxide (DCP) grade Retilox 40 SAP, both used as additives for reactive extrusion, were purchased in local market.

2.2 Design of experiments (DOE)

The effects of the reverse mixture elements (RME) and the feed rate (FR) in the properties of the PLA/PBAT (70/30, wt.%) blends were assessed using the Simple Factorial 2^2 design of experiment (DOE). Table 1 shows the experimental matrix and respective actual values of RME and FR. This DOE investigation was applied for two conditions of processing: non-reactive and reactive extrusion, which were coded as NAD (the additives MA and DCP were not used) and AD (the additives MA and DCP were used). The experimental code used for the blend identification is X/Y-W where X and Y are the actual values of RME and FR (Table 1), and W can assume the code "AD" or "NAD" for reactive and non-reactive extrusion, respectively. For AD blends the amount of MA and DCP were, respectively, 1.0 and 2.0 phr (parts per hundred of resin) in relation to PLA, which corresponds to 1.0 and 1.9 wt%, respectively. Additionally, pristine polymers PLA and PBAT were also processed under RME/FR conditions of 0/2.5 (PLA–0/2.5 and PBAT–0/2.5) and 2/5.2 (PLA–2/5.2 and PBAT–2/5.2) to be used as references of comparison to the blends.

Table 1. DOE matrix of Simple Factorial 2^2.

Code level		Actual value	
RME	FR	RME	FR
-1	-1	0	2.5 kg.h^{-1}
-1	1	0	5.2 kg.h^{-1}
1	-1	2	2.5 kg.h^{-1}
1	1	2	5.2 kg.h^{-1}
0	0	1	3.9 kg.h^{-1}

Note: Center point (RME:0 and FR:0): three replicates for NAD and two replicates for AD.

The response variables were impact resistance (IR), elastic modulus (EM), yield stress (YS), temperature at maximum degradation rate (T_{max}), cold crystallization temperature (T_{cc}), cold crystallization enthalpy (ΔH_c), melting temperatures (Tm_1 and Tm_2), melting enthalpy (ΔH_f), and degree of crystallinity (χc).

The DOE analysis was performed using Statistics v.10 software at the 95% confidence level (p-values < 0.05), and the results were presented in this study as Pareto Charts and graphics of means. The Pareto chart is a bar graphic that displays the contribution of the factors and/ or their interactions in a decrease order of importance, and contains a line related to the p-value of 0.05. Any effect and/interaction that extends this reference line affects the response variable.

2.3 Blends preparation

Before the extrusion process, PLA and PBAT were dried in a forced-air oven at 60°C for 20h. The blends and pristine polymers were processed using a Tecktril DCT-20 co-rotating twin screw extruder (L/D: 36 and D:20 mm) with screw speed of 200 rpm, and temperature profile of 90 /180/190/190/190/200/200/200/190ºC.

After extrusion, the materials were pelletized. The test specimens were prepared by injection molding in the Arburg machine model 270S with a temperature profile of 200/200/190/180/180ºC, 1500 bar injection pressure, molding temperature of 30°C, and cooling time of 30s. Similar to extrusion, the PLA/PBAT blends and PLA and PBAT were dried in a forced-air oven at 60°C for 20h before being submitted to the injection. The screw profiles used are described in Figure 1.

2.4 Characterizations

Infrared spectra (FTIR) were recorded on a PerkinElmer spectrometer, model Spectrum One, working in the attenuated total reflectance (ATR) mode, in a range of 4000–515 cm^{-1}. The absorbance height ratios were measured using the baseline 1910 – 810 cm^{-1}. The impact resistance (IR) was evaluated with Izod impact test (ASTM D256). The specimens were subjected to the impact of a

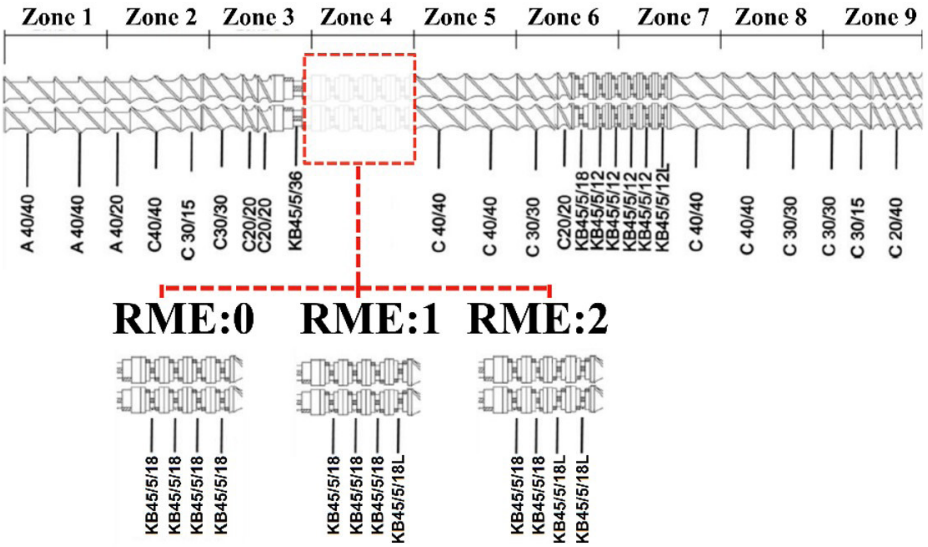

Figure 1. Screw profiles used. Zones: 1-9.

2 J pendulum at an angle of 90°, on CEAST equipment, model Resil Impactor. Tensile properties were determined by the Universal Testing Machine, model EMIC DL3000, according to ASTM D638, with a speed of 5 mm.min^{-1}. Thermogravimetric Analysis (TGA) was conducted in a Q500 analyzer, TA Instruments, under an atmosphere of N_2, from 30 to 700°C, and heating rate of 20°C.min^{-1}. From each thermogram, it was read the temperature at the maximum mass loss rate (Tmax). The effect of the process parameters on the crystallization behavior of the blends was evaluated using a DSC Analyzer, model 2910 MDSC, heating the samples in nitrogen atmosphere from 40 to 210°C at 5°C.min^{-1}. This protocol was set to investigate the effect of the process parameters on the crystallization of the polymers. The crystallinity of pristine PLA and the PLA presented in the blends were determined by Equation 1, and the crystallinity of pristine PBAT was determined using Equation 2.

$$\chi_{PLA} = 100 \times \frac{\Delta Hf - \Delta Hc}{wPLA * 93} \quad (1)$$

where χ_{PLA} is the crystallinity degree of PLA, w_{PLA} is the PLA content, ΔHf is the melting enthalpy of PLA in J.g^{-1} and ΔHc is the cold crystallization enthalpy of PLA in J.g^{-1} [13,22,23].

$$\chi_{PBAT} = 100 \times \frac{\Delta Hf}{114} \quad (2)$$

where χ_{PBAT} is crystallinity degree of PBAT, ΔHf is the melting enthalpy of PBAT in J.g^{-1} and ΔHc is the cold crystallization enthalpy of PBAT in J.g^{-1}[13,22,23]. The morphology of the blends was observed using a scanning electron microscope (SEM), model JEOL JSM-6510. The standard dumbbell test specimens (Type 1, ASTM D638) were cryogenically fractured in the "neck region" to allow observing the disperse phase in the transverse and parallel directions in relation to the length of the sample (Lo), based on the Standard ASTM D638. Then, the cryofractured surface were sputter-coated with gold before analysis.

3. Results and Discussions

3.1 SEM micrographs

Figure 2 presents the images from SEM taken in the fractured surface of PLA/PBAT blends. As expected, both the NAD and AD blends show phase-separated morphology typical of immiscible polymers[7,8].

Analyzing the images of the NAD blends (Figure 2a-j), one observes that the dispersed phase of PBAT has a fibrillar form oriented with the parallel direction, although some droplets and circular cavities are also visible. On the other side, the dispersed phase of all AD blends presents the droplet shape in the parallel and transverse directions (Figure 2k-t). Additionally, both RME and FR factors did not affect the morphologies of the disperse phase of the AD and NAD blends. Similar droplet morphology with dimensions around 0.3 – 0.5 mm for PLA/PLA-g-MA/PBAT was reported by Rigolin et al.[11], that is, lower than that observed in this study.

3.2 Fourier-transform infrared spectroscopy (FT-IR)

FT-IR analysis was used to investigate whether the addition of MA and DCP for reactive extrusion and/or FR and RME have generated, or not, some occurrence of degradation in PLA/PBAT blends. Figure 3 presents a comparison among the spectra of the PLA/PBAT blends, and the PLA and PBAT without processing (coded "pellet").

The most important bands that characterize sample "PLA pellet" are at around 1752 cm^{-1} (carbonyl elongation vibration C–O), 1453 cm^{-1} (CH_3 asymmetric bending vibration), 1182, and 1090 cm^{-1} (symmetrical elongation of C–O–C), and 872 cm^{-1} (C-COOO stretching)[24-27]. Further, there are two bands at around 2800-3000 cm^{-1} relating to the symmetric stretching vibration of the axial CH groups in saturated hydrocarbons[13,28]. The presence of the bands around 3298 cm^{-1} (O–H)[27] and 1636 cm^{-1} (H–O–H)[13] can be associate with the presence of moisture in the "PLA pellet" sample. For sample "PBAT pellet," the most relevant bands are located at the regions 727 cm^{-1}, 1712 cm^{-1}, and 2960 cm^{-1},

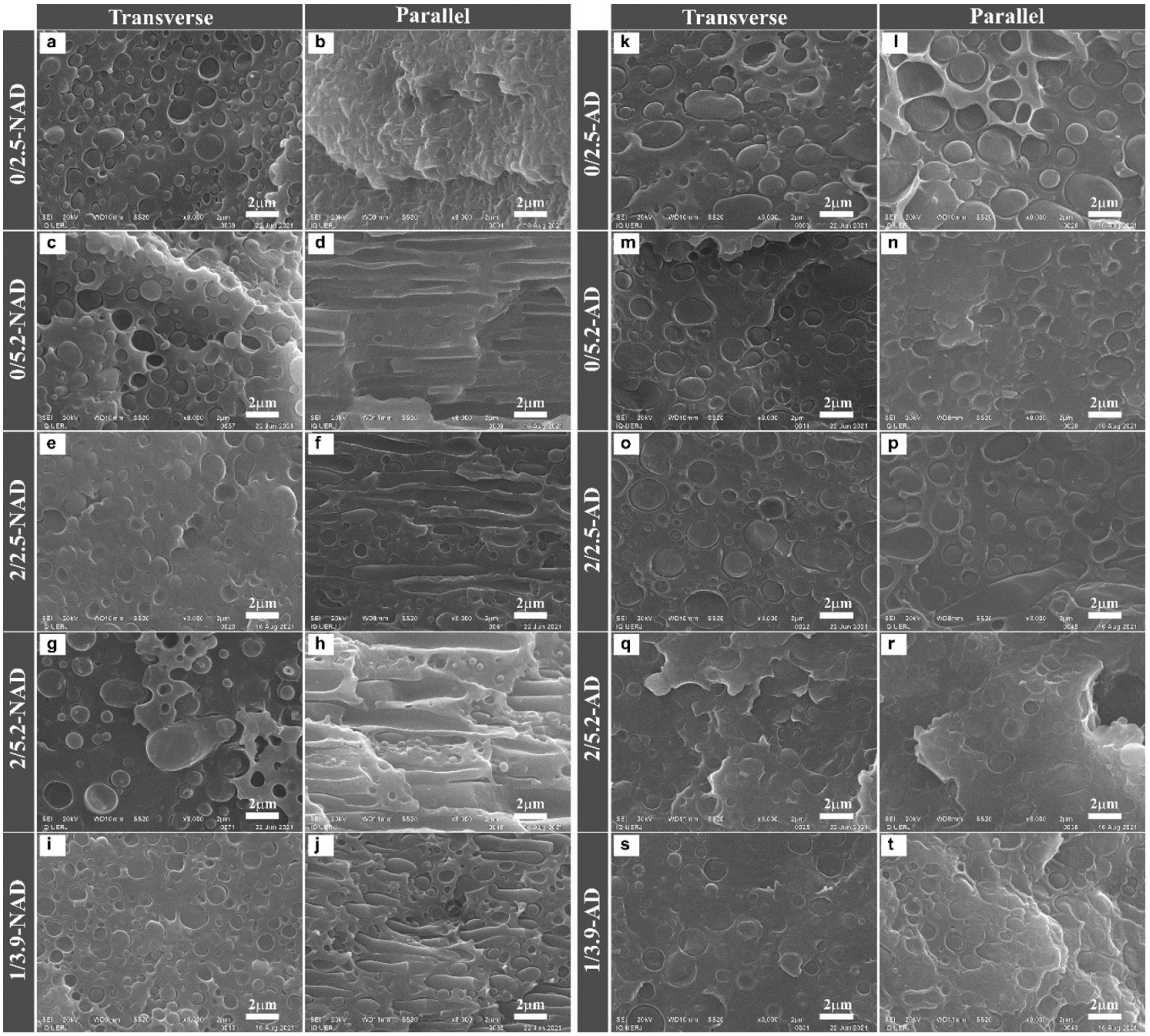

Figure 2. SEM images of PLA/PBAT blends at 8000x of magnification (2 μm) taken in the transverse and parallel melt flow directions of: (a-b) 0/2.5-NAD, (c-d) 0/5.2-NAD, (e-f) 2/2.5-NAD, (g-h) 2/5.2-NAD, (i-j) 1/3.9-NAD, (k-l) 0/2.5-AD, (m-n) 0/5.2-AD, (o-p) 2/2.5-AD, (q-r) 2/5.2-AD, and (s-t) 1/3.9-AD.

which are assigned, respectively, to the vibration in the CH plane of the benzene ring[24,25], C–O stretch vibration[26] and CH stretching in the aliphatic and aromatic portions[28].

It is observed that NAD and AD blends present all the aforementioned bands of the PBAT and PLA pellet samples, except the bands at around 3298 cm^{-1} and 1636 cm^{-1}. This means that the bands of OH groups (around the 3500 cm^{-1})[27] associated with the degradation of PLA by mechanism hydroxyl groups[23] were not identified. Additionally, the band characteristic of the ester carbonyl group (1751 cm^{-1}) did not shift to the region of the acid carbonyl group (around 1756 cm^{-1})[29]. This result indicates that PLA did not suffer hydrolysis degradation, which is an expected behavior, since both the PLA and PBAT were dried in an air circulation oven for moisture removal before being processed. However, PLA can suffer thermo-mechanical and thermo-oxidative degradation caused by high temperature and shear in the oxygen presence during the extrusion process. Since this degradation process breaks the polymer chain, producing more ester group, it can be investigated by the absorbance height ratios related to carbonyl groups[30], that is, 1752 cm^{-1} (C=O stretching), 1182 cm^{-1} (C–O stretching), and 1090 cm^{-1} (C–O stretching) in relation to the band of CH_3 deformation at 1453 cm^{-1} (Figure 4). Using "PLA pellet" data as a reference, the comparison shown in Figure 4 indicates that both PLA processed (PLA-0/2.5 and PLA-2/5.2) and PLA into the NAD and AD blends suffered thermo-mechanical and/or thermo-oxidative degradations, being this process more pronounced for the blends produced by non-reactive extrusion. It is important to highlight that this comparison is just a qualitative way to evaluate the occurrence of the degradation process.

Unlike other studies[31,32], the characteristic bands of MA corresponding to the stretch of C = O in the ranges of 1830 – 1800 cm^{-1} and 1775 – 1740 cm^{-1} [33] were not identified. One reason is the overlapping of the bands (region at1775 – 1740 cm^{-1}) and/or the lower intensity of the band at

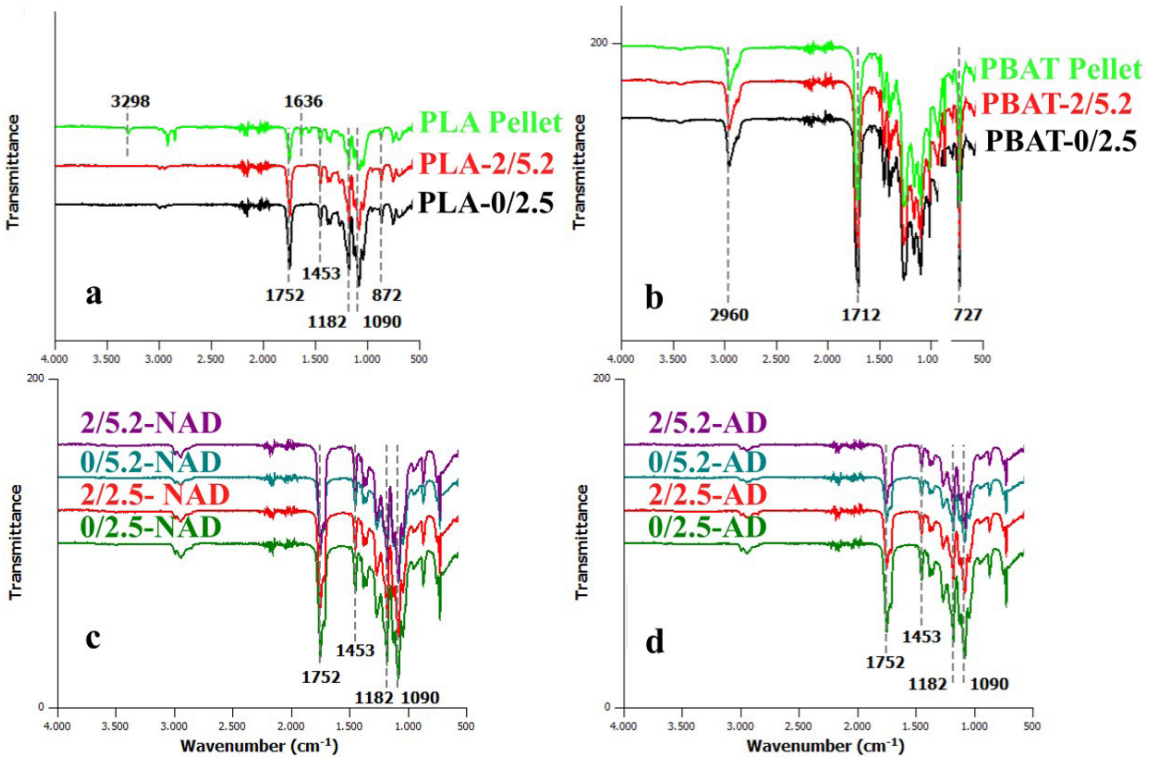

Figure 3. FT-IR spectra for: (a) PLA pellet, PLA–2/5.2, and PLA–0/2.5, (b) PBAT pellet, PBAT–2/5.2, (c) 2/5.2-NAD, 0/5.2-NAD, 2/2.5-NAD, 0/2.5-NAD, and (d) 2/5.2-AD, 0/5.2-AD, 2/2.5-AD, 0/2.5-AD.

around 1830 – 1800 cm^{-1} due to the small content of maleic anhydride (1.0 wt.%) in the AD blends.

3.3 Thermal properties by TGA

Table 2 shows the values of temperature at the maximum degradation rate (T_{max}) for AD and NAD blends, PLA and PBAT processed under 0/2.5 and 2/5.2 conditions, and PLA and PBAT pellet. To better illustrate this thermal property, Figure 5 shows the comparison of the DTG curves of PLA–0/2.5, PBAT–0/2.5, 0/2.5-AD, and 0/2.5-NAD (Figure 5a) and PLA–2/5.2, PBAT–2/5.2, 2/5.2-AD, and 2/5.2-NAD (Figure 5b).

Using T_{max} value of "PLA and PBAT pellet" as a reference (Table 3), one observes a reduction of the T_{max} values just for the PLA–0/2.5 and PLA–2/5.2, being the values of processed PBAT remained the same as the PBAT pellet one. Furthermore, a reduction in the T_{max} values of NAD and AD blends was also observed, being this reduction more pronounced than the one of processed PLA. This shift of T_{max} for lower values of temperature corroborates the finds of the FTIR analysis, which indicated that PLA suffered some degradation process, being this process seemingly more pronounced for the PLA/PBAT blend produced by non-reactive extrusion. This result is interesting since it suggests a better thermal resistance of the PLA/PBAT blend produced from reactive extrusion. According to the literature[2], blends with better phase interaction tend to show higher thermal stability. Regarding the effect of the extrusion process parameters, the analysis of DOE for AD and NAD blends resulted that both RME and FR did not cause any influence on the Tmax since all p-values were higher than 0.05.

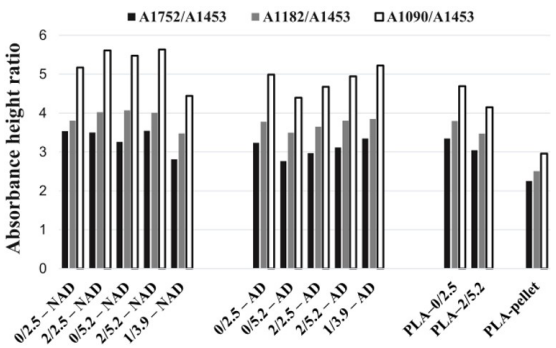

Figure 4. Comparison of the absorbance height ratio among the PLA/PBAT blends produced from reactive (AD blends) and non-reactive extrusion (NAD blends), PLA-0/2.5, PLA-2/5.2, and PLA-pellet.

3.4 Thermal properties by DSC

Figures 6 and 7 show the DSC curves for the pristine polymers and blends, respectively. The thermal properties obtained from the DSC analysis are shown in Table 3.

The analysis of curves in Figure 6 shows that the curve of PLA pellet did not exhibit a peak related to cold crystallization, while the PLA-0/2.5 and PLA-2/5.2 do due to a thermal history of processing. Different to PLA pellet, both PLA and PLA-2/5.2 showed an endothermic transition characterized by a bimodal melting peak that occurs due to

Table 2. Temperature at maximum degradation rate (T_{max}) of the PLA/PBAT blends produced from non-reactive extrusion (NAD blends) and reactive (AD blends), PLA and PBAT processed under 0/2.5 and 2/5.2 conditions, and PLA and PBAT pellets.

Sample code	T_{max} (°C)	Sample code	T_{max} (°C)	Sample code	T_{max} (°C)
PLA–0/2.5	383	0/2.5-NAD	365	0/2.5-AD	369
PBAT-0/2.5	419				
2/2.5-NAD		0/5.2-NAD	350	0/5.2-AD	373
		347	2/2.5-AD	369	
PLA–2/5.2	384	2/5.2-NAD	359	2/5.2-AD	362
PBAT-0/2.5	420				
		1/3.9-NAD	362 ± 5	1/3.9-AD	365 ± 4
PLA pellet	391				
PBAT pellet	420				

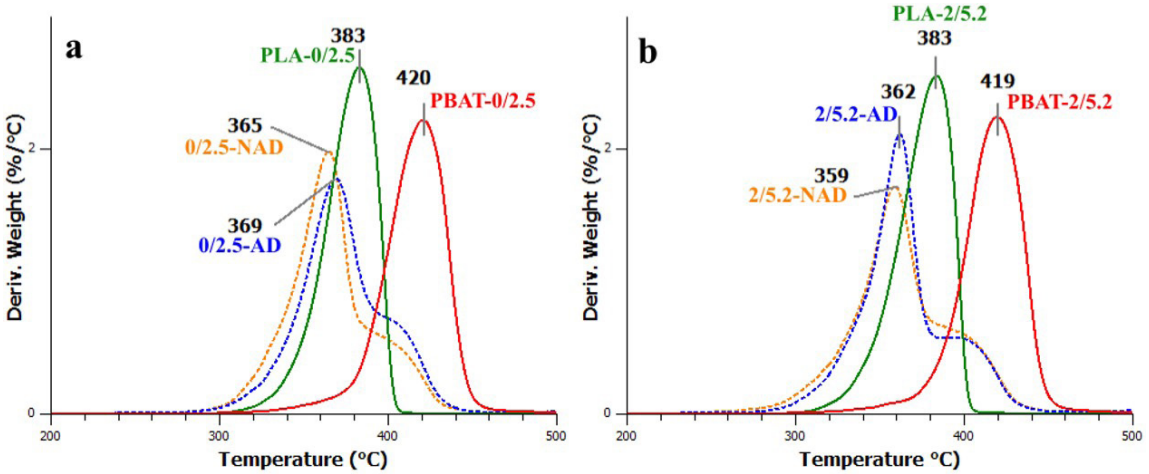

Figure 5. DTG curves comparison of PLA, PBAT, PLA/PBAT blends produced from non-reactive extrusion (NAD blends) and reactive (AD blends) under (a) 0/2.5 condition and (b) under 2/5.2 condition.

the heterogeneity of the crystal formation[34,35]. No significant differences were observed for any of the PBAT sample. In fact, one can observe in Table 3 that PLA-0/2.5 and PLA-2/5.2 showed a reduction in χc, while that PBAT-0/2.5 and PBAT-2/5.2 did not, compared to the χc values of PLA pellet and PBAT pellet, respectively.

In contrast to the PBAT-0/2.5 and PBAT-2/5.2 (Figure 6), a peculiar result is observed in the DSC curves of the blends (Figure 7a, b), that is, the disappearance of the peak referring to the melting of PBAT crystals, which that should have occurred at temperatures around 125°C (Figure 4). This result indicates that the PBAT phase is in the amorphous state. One reason that can explain this find is that the lower chain flexibility of PLA can hinder the mobility of PBAT chains, making it difficult to crystallize[13]. The comparison of the values of χc of PLA (Table 3) shows that both NAD and AD blends presented lower χc than PLA pellet and slightly lower than PBAT-0/2.5 and PBAT-2/5.2, which suggests that the presence of the PBAT phase disturbs the PLA to crystalize[27,32].

The analysis of the experiment for NAD blends, for all properties presented in Table 3, resulted that only the cold crystallization temperature (T_{cc}) was affected by the extrusion process parameters. Figure 8 shows the Pareto Chart and the Graphic of means for T_{cc} obtained from the design of experiment.

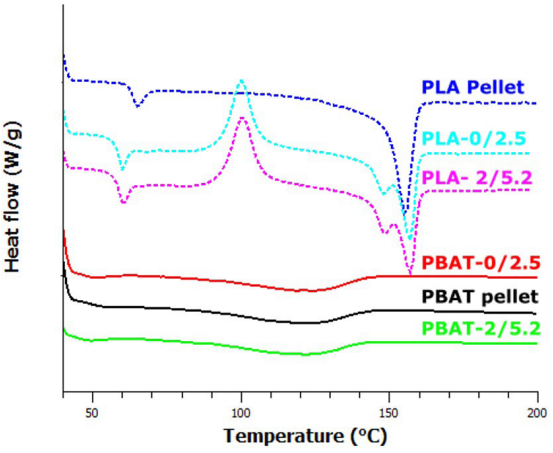

Figure 6. DSC curves of PLA pellet, PBAT pellet, PLA-0/2.5, PLA-2/5.2, PBAT-0/2.5, and PBAT-2/5.2.

It is observed that RME had a slight effect (p-value: 0.039) on the T_{cc} property, that is, the use of two reverse mixture elements contributes to reducing the T_{cc} of the blends. Furthermore, one can observe that exists a trend of reduction in the T_{cc} values of NAD blends compared with the PLA–0/2.5 and PLA–2/5.2, as well as AD blends.

Table 3. Test results of T_{cc}, ΔH_c, Tm_1, Tm_2, ΔH_f and χc.

Samples Code	T_{cc} (J.g^{-1})	ΔH_c (J.g^{-1})	Tm_1 (°C)	Tm_2 (°C)	ΔH_f (J.g^{-1})	χc PBAT (%)	χc PLA (%)
PLA pellet	-	-	155	-	28	-	30
PBAT pellet	-	-	123	-	11	10	-
PLA–0/2.5	100	18	148	157	22	-	6
PLA–2/5.2	101	20	149	157	24	-	6
PBAT–0/2.5	-	-	121	-	11	10	-
PBAT–2/5.2	-	-	125	-	11	10	-
0/2.5 – NAD	99	13	146	153	16	-	5
0/5.2 – NAD	96	12	145	152	15	-	3
2/2.5 – NAD	86	12	134	142	15	-	5
2/5.2 – NAD	94	12	142	150	15	-	5
1/3.9 – NAD	94 ± 6	12 ±1	142 ±5	149 ±5	15 ± 1	-	4 ±1
0/2.5 – AD	98	15	145	155	18	-	3
0/5.2 – AD	98	14	145	155	17	-	5
2/2.5 – AD	96	14	143	154	17	-	5
2/5.2 – AD	100	15	145	156	17	-	3
1/3.9 – AD	98 ± 2	15 ±1	145±1	155 ±1	17 ± 1	-	4 ±1

Legend: T_{cc}: cold crystallization temperature; ΔHc: cold crystallization enthalpy; Tm_1 and Tm_2: first and second temperatures of the bimodal melting peak of PLA; ΔHf: melting enthalpy; and χc: degree of crystallinity.

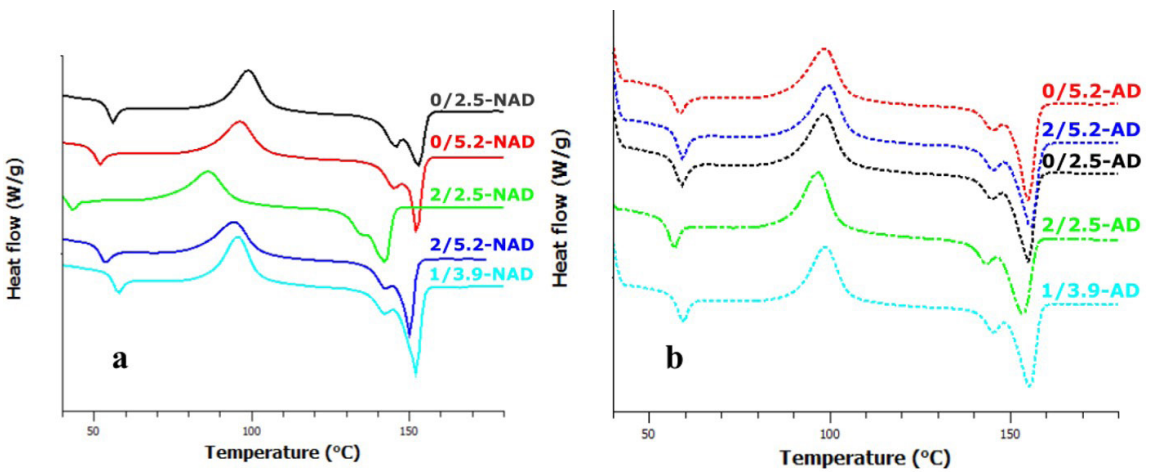

Figure 7. DSC curves for PLA/PBAT blends produced from (a) non-reactive extrusion (NAD blends) and (b) reactive extrusion (AD blends).

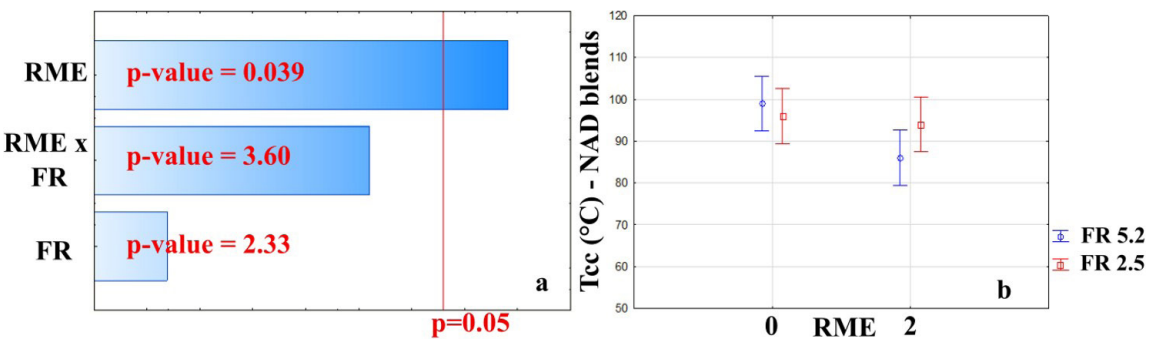

Figure 8. Pareto's chart and Plot of Means for Tcc of NAD blends generated from the analysis of experiment.

According to literature[36], the exothermic crystallization peak during heating occurs due to the reorganization of amorphous into crystalline domains, caused by the increase in flexibility and macromolecular mobility generated by the temperature rise. Therefore, based on this finding, one can infer that the high shear generated by the use of the two RME produced a "arrange" of polymer chains that facilitated their movement. Regarding AD blends, the analysis of the

experiment resulted that both RME and FR did not affect none of the thermal properties shown in Table 3 since all p-values were higher than 0.05.

3.5 Mechanical properties

Table 4 presents the experimental data of impact resistance (IR), initiation (IE) and crack propagation (PE) energies, elastic modulus (EM), and yield stress (YS).

The PLA/PBAT unmodified blends (NAD blends) showed higher standard deviation of all properties, as can be seen in the comparisons between 1/3.9–NAD and 1/3.9–AD blends. This tendency of higher variability of NAD blends can be attributed to the fact that the immiscibility of PLA and PBAT leads to the production of non-uniform morphology[14].

Regarding the Izod impact test, as expected, the blends of the two groups had a much higher IR values than the value of pristine PLA, showing the role of the PBAT to improve the toughness. One can observe that the AD blends presented higher values of IR than the NAD ones. The same behavior was found for IE and PE. Further, one can observe that the energies to initiate the crack are always higher than the propagation values regardless the group of blends. All the previous results indicated that the blends compatibilized by reactive extrusion showed a higher toughness behavior. This result suggests that a better interaction between the phases of PLA and PBAT occurred during reactive extrusion. The better toughness behaviour of AD blends was the opposite of the reported by Rigolin et al.[11]. With respect to the effect of RME and FR on the toughness behavior of the two groups of blends, the analysis of experiment resulted in p-value higher 0.05, meaning that the two factors did not lead to significant changes in the IR, IE, and PE properties.

In relation to tensile properties, although there is a tendency for reduction of YS values for AD blends compared to NAD ones, the same behavior was not seen for stiffness, given that the difference in EM's values between the two groups was not so significant. Being precise, changes between the two groups were observed only for experiments 0/2.5 and 1/3.9, that is, the EM of 0/2.5–NAD was 10% higher than the value of 0/2.5–AD, while the EM of 1/3.9–NAD blend was 6% lower than the value of 1/3.9–AD. This find is the opposite of Rigolin et al.[11] study, which reported a decrease in elastic modulus for the blends produced by reactive extrusion.

Figure 9 shows the Pareto Chart and the Graphic of means for EM property obtained from the design of experiment.

Table 4. Mechanical Properties of PLA, PBAT and PLA/PBAT blends.

Code	IR (J/m)	IE (J,10^{-3})	PE (J,10^{-3})	EM (MPa)	YS (MPa)
PLA (0/2.5)	27 ± 2	78 ± 10	15 ± 3	1895 ± 122	58 ± 1
PLA (2/5.2)	26 ± 5	73 ± 16	15 ± 3	1852 ± 122	56 ± 1
PBAT (0/2.5)		Specimens did not break		54 ± 9	6 ± 0
PBAT (2/5.2)		Specimens did not break		54 ± 3	6 ± 0
0/2.5 – NAD	70	207	25	1788	40
0/5.2 – NAD	88	277	20	1538	38
2/2.5 – NAD	93	279	20	1602	39
2/5.2 – NAD	90	276	24	1583	38
1/3.9 – NAD	73 ± 11	229 ± 38	17 ± 7	1535 ± 4	39 ± 1
0/2.5 – AD	108	327	27	1610	35
0/5.2 – AD	100	295	32	1542	35
2/2.5 – AD	108	333	27	1603	35
2/5.2 – AD	110	330	22	1550	34
1/3.9 – AD	95 ± 2	296 ± 4	21 ± 3	1624 ± 1	34 ± 1

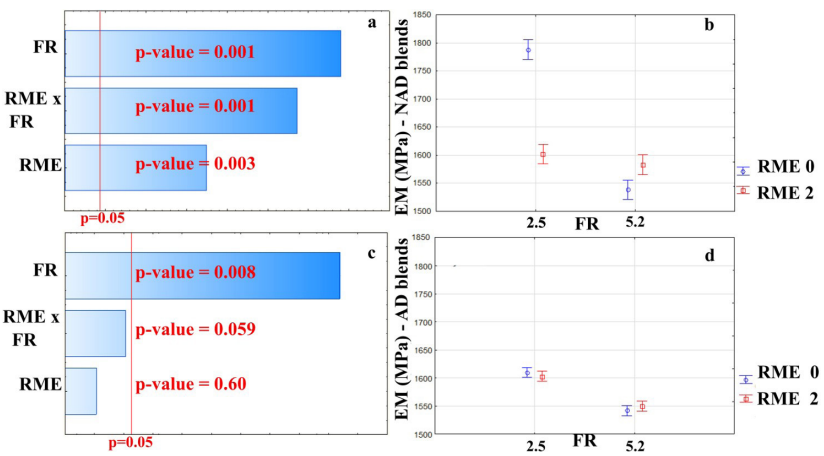

Figure 9. Elastic Modulus (EM) of NAD blends: (a)Pareto Chart and (b) Plot of means, and AD blends: (c) Pareto Chart and (d) Plot of means.

It is observed in the Pareto Chart (Figure 9a) that both RME and FR parameters and the interaction between them was significant for the NAD blend group (p-values are higher than 0.05). According to the means plot (Figure 9b), EM decreases and FR increases, but this reduction is more pronounced when there are no reverse mixture elements (Figure 9b – blue, RME: -1, actual value of 0) on the extruder profile. Alternatively, the Pareto Chart of AD blends (Figure 9c) shows that only FR influenced the EM property, producing a decrease in it as the factor level increased (Figure 9d). This result reveals how effective the reactive extrusion was since the AD blends were less susceptible to the effect of process parameters. One reason that explains this result is the fact that the addition of MA and DCP led to a greater interaction between PLA and PBAT phases, which was responsible for the higher stability of the melt morphology during processing. In contrast with EM, the analysis of experiment revealed that FR and RME, as well as their interaction, did not affect the YS for both AD and NAD blends (p-values > 0.05). Previous findings related to Izod impact and tensile properties mean that, depending on the processing conditions, PLA and PBAT compatibilized blends in the reactive extrusion can lead to the production of materials with higher toughness, simultaneously, without significantly lost its stiffness behavior.

4. Conclusions

This study revealed that a better interaction between the PLA and PBAT phases occurred by reactive extrusion. The FTIR and TGA analysis showed that pristine polymers and their blends suffered a slight thermo-mechanical and thermo-oxidative degradation that does not compromise the mechanical properties. An increase in the impact behavior of the blends was observed, without significantly lost in the rigidity behavior. The feed rate (FR) and reverse mixture elements (RME) affected the EM property for NAD blends, while only FR affected the AD blends. According to the thermal properties of the DSC, the AD blends were also more resistant and less sensitive to changes in processing. The T_{cc} of the NAD blend decreased as the number of reverse mixing elements increased and this behavior did not repeat for AD blends. It can be concluded that blends produced by reactive extrusion presented better mechanical and thermal behavior.

5. Author's Contribution

- **Conceptualization** – Virnna Cristhielle Santana Barbosa; Ana Maria Furtado de Sousa; Ana Lúcia Nazareth da Silva.
- **Data curation** – Virnna Cristhielle Santana Barbosa.
- **Formal analysis** – Virnna Cristhielle Santana Barbosa.
- **Funding acquisition** – Ana Maria Furtado de Sousa; Ana Lúcia Nazareth da Silva.
- **Investigation** – Virnna Cristhielle Santana Barbosa.
- **Methodology** – Ana Maria Furtado de Sousa; Ana Lúcia Nazareth da Silva.
- **Project administration** – Ana Lúcia Nazareth da Silva.
- **Resources** – Virnna Cristhielle Santana Barbosa; Ana Maria Furtado de Sousa; Ana Lúcia Nazareth da Silva.
- **Software** – Not applicable.
- **Supervision** – Ana Maria Furtado de Sousa; Ana Lúcia Nazareth da Silva.
- **Validation** – Virnna Cristhielle Santana Barbosa; Ana Maria Furtado de Sousa; Ana Lúcia Nazareth da Silva.
- **Visualization** – Virnna Cristhielle Santana Barbosa.
- **Writing – original draft** – Virnna Cristhielle Santana Barbosa.
- **Writing – review; editing** – Ana Maria Furtado de Sousa; Ana Lúcia Nazareth da Silva.

6. Acknowledgements

We would like to thank the Conselho Nacional de Desenvolvimento Científico e Tecnológico (BR) – CNPq [PQ-2/2018: 305007/2018-1 and PQ-2/2021: 309461/2021-9], Fundação Carlos Chagas Filho de Amparo à Pesquisa do Estado do Rio de Janeiro – FAPERJ [APQ1 2019: E-26/010.001927/2019], and Coordenação de Aperfeiçoamento de Pessoal de Nível Superior – Brasil (CAPES) [Financing code 001, and the PhD Scholarship received by Virnna Barbosa].

7. References

1. Urquijo, J., Aranburu, N., Dagréou, S., Guerrica-Echevarría, G., & Eguiazábal, J. I. (2017). CNT-induced morphology and its effect on properties in PLA/PBAT-based nanocomposites. *European Polymer Journal*, *93*, 545-555. http://dx.doi.org/10.1016/j.eurpolymj.2017.06.035.
2. Sangeetha, V. H., Deka, H., Varghese, T. O., & Nayak, S. K. (2016). State of the art and future prospectives of poly(lactic acid) based blends and composites. *Polymer Composites*, *39*(1), 81-101. http://dx.doi.org/10.1002/pc.23906.
3. Jian, J., Xiangbin, Z., & Xianbo, H. (2020). An overview on synthesis, properties and applications of poly(butylene-adipate-co-terephthalate)–PBAT. *Advanced Industrial and Engineering Polymer Research*, *3*(1), 19-26. http://dx.doi.org/10.1016/j.aiepr.2020.01.001.
4. Zhang, Y., Jia, S., Pan, H., Wang, L., Bian, J., Guan, Y., Li, B., Zhang, H., Yang, H., & Dong, L. (2021). Effect of glycidyl methacrylate-grafted poly(ethylene octene) on the compatibility in PLA/PBAT blends and films. *Korean Journal of Chemical Engineering*, *38*(8), 1746-1755. http://dx.doi.org/10.1007/s11814-021-0809-1.
5. Dil, E. J., Carreau, P. J., & Favis, B. D. (2015). Morphology, miscibility, and continuity development in poly(lactic acid)/poly(butylene adipate-co-terephthalate) blends. *Polymer*, *68*, 202-212. http://dx.doi.org/10.1016/j.polymer.2015.05.012.
6. Mohammadi, M., Heuzey, M.-C., Carreau, P. J., & Taguet, A. (2021). Morphological properties of PLA, PBAT, and PLA/PBAT blend nanocomposites containing CNCs. *Nanomaterials*, *11*(4), 857. http://dx.doi.org/10.3390/nano11040857. PMid:33801672.
7. Su, S. (2021). Prediction of the Miscibility of PBAT/PLA blends. (2021). *Polymers*, *13*(14), 2339. http://dx.doi.org/10.3390/polym13142339. PMid:34301096.
8. Rebelo, R. C., Gonçalves, L. P. C., Fonseca, A. C., Fonseca, J., Rola, M., Coelho, J. F. J., Rola, F., & Serra, A. C. (2022). Increased degradation of PLA/PBAT blends with organic acids and derivatives in outdoor weathering and marine

environment. *Polymer*, *256*, 125223. http://dx.doi.org/10.1016/j.polymer.2022.125223.

9. Lin, S., Guo, W., Chen, C., Ma, J., & Wang, B. (2012). Mechanical properties and morphology of biodegradable poly(lactic acid)/poly(butylene adipate-co-terephthalate) blends compatibilized by transesterification. *Materials & Design*, *36*, 604-608. http://dx.doi.org/10.1016/j.matdes.2011.11.036.
10. Arruda, L. C., Magaton, M., Bretas, R. E. S., & Ueki, M. M. (2015). Influence of chain extender on mechanical, thermal, and morphological properties of blown films of PLA/ PBAT blends. *Polymer Testing*, *43*, 27-37. http://dx.doi.org/10.1016/j.polymertesting.2015.02.005.
11. Rigolin, T. R., Costa, L. C., Chinelatto, M. A., Muñoz, P. A. R., & Bettini, S. H. P. (2017). Chemical modification of poly(lactic acid) and its use as matrix in poly(lactic acid) poly(butylene adipate- co -terephthalate) blends. *Polymer Testing*, *63*, 542-549. http://dx.doi.org/10.1016/j.polymertesting.2017.09.010.
12. Choudhury, G. S., & Gautam, A. (1998). Comparative study of mixing elements during twin-screw extrusion of rice flour. *Food Research International*, *31*(1), 7-17. http://dx.doi.org/10.1016/S0963-9969(98)00053-2.
13. Al-Itry, R., Lamnawar, K., & Maazouz, A. (2012). Improvement of thermal stability, rheological and mechanical properties of PLA, PBAT and their blends by reactive extrusion with functionalized epoxy. *Polymer Degradation & Stability*, *97*(10), 1898-1914. http://dx.doi.org/10.1016/j.polymdegradstab.2012.06.028.
14. Hongdilokkul, P., Keeratipinit, K., Chawthai, S., Hararak, B., Seadan, M., & Suttiruengwong, S. (2015). A study on properties of PLA/PBAT from blown film process. *IOP Conference Series. Materials Science and Engineering*, *87*, 012112. http://dx.doi.org/10.1088/1757-899X/87/1/012112.
15. Silva, D., Kaduri, M., Poley, M., Adir, O., Krinsky, N., Shainsky-Roitman, J., & Schroeder, A. (2018). Biocompatibility, biodegradation, and excretion of polylactic acid (PLA) in medical implants and theranostic systems. *Chemical Engineering Journal*, *340*, 9-14. http://dx.doi.org/10.1016/j.cej.2018.01.010. PMid:31384170.
16. Zheng, J., Choo, K., & Rehmann, L. (2015). The effects of screw elements on enzymatic digestibility of corncobs after pretreatment in a twin-screw extruder. *Biomass and Bioenergy*, *74*, 224-232. http://dx.doi.org/10.1016/j.biombioe.2015.01.022.
17. Ding, Y., Abeykoon, C., & Perera, Y. S. (2022). The effects of extrusion parameters and blend composition on the mechanical, rheological, and thermal properties of LDPE/PS/PMMAternary polymer blends. *Advances in Industrial and Manufacturing Engineering*, *4*, 100067. http://dx.doi.org/10.1016/j.aime.2021.100067.
18. Oliveira, A. G., Silva, A. L. N., Sousa, A. M. F., Leite, M. C. A. M., Jandorno, J. C., & Escócio, V. A. (2016). Composites based on green high-density polyethylene, polylactide and nanosized calcium carbonate: effect of the processing parameter and blend composition. *Materials Chemistry and Physics*, *181*, 344-351. http://dx.doi.org/10.1016/j.matchemphys.2016.06.068.
19. Vergnes, B., Barrès, C., & Tayeb, J. (1992). Computation of residence time and energy distributions in the reverse screw element of a twin-screw extrusion-cooker. *Journal of Food Engineering*, *16*(3), 215-237. http://dx.doi.org/10.1016/0260-8774(92)90035-5.
20. Ambrósio, J. D., Pessan, L. A., Larocca, N. M., & Hage, E., Jr. (2010). Influência das condições de processamento na obtenção de blendas PBT/ABS. *Polímeros: Ciência e Tecnologia*, *20*(4), 315-321. http://dx.doi.org/10.1590/s0104-14282010005000051.
21. Yeh, A.-I., Hwang, S.-J., & Guo, J.-J. (1992). Effects of screw speed and feed rate on residence time distribution and axial mixing of wheat flour in a twin-screw extruder. *Journal of Food Engineering*, *17*(1), 1-13. http://dx.doi.org/10.1016/0260-8774(92)90061-A.
22. Kamal, M. R., Utracki, L. A., & Mirzadeh, A. (2014) *Rheology of polymer alloys and blends.* In L. A. Utracki, & C. A. Wilkie (Eds.), *Polymer blends handbook* (pp. 725-873). Netherlands: Springer. http://dx.doi.org/10.1007/978-94-007-6064-6_9
23. Al-Itry, R., Lamnawar, K., Maazouz, A., Billon, N., & Combeaud, C. (2015). Effect of the simultaneous biaxial stretching on the structural and mechanical properties of PLA, PBAT and their blends at rubbery state. *European Polymer Journal*, *68*, 288-301. http://dx.doi.org/10.1016/j.eurpolymj.2015.05.001.
24. Ding, Y., Feng, W., Lu, B., Wang, P., Wang, G., & Ji, J. (2018). PLA-PEG-PLA tri-block copolymers: effective compatibilizers for promotion of the interfacial structure and mechanical properties of PLA/PBAT blends. *Polymer*, *146*, 179-187. http://dx.doi.org/10.1016/j.polymer.2018.05.037.
25. Weng, Y.-X., Jin, Y.-J., Meng, Q.-Y., Wang, L., Zhang, M., & Wang, Y.-Z. (2013). Biodegradation behavior of poly(butylene adipate-coterephthalate)(PBTA), poly(lactic acid)(PLA), and their blend under soil conditions. *Polymer Testing*, *32*(5), 918-926. http://dx.doi.org/10.1016/j.polymertesting.2013.05.001.
26. Rosenberger, A. G., Dragunski, D. C., Muniz, E. C., Módenes, A. N., Alves, H. J., Tarley, C. R. T., Machado, S. A. S., & Caetano, J. (2019). Electrospinning in the preparation of an electrochemical sensor based on carbon nanotubes. *Journal of Molecular Liquids*, *298*, 112068. http://dx.doi.org/10.1016/j.molliq.2019.112068.
27. Wang, L.-F., Rhim, J.-W., & Hong, S.-I. (2016). Preparation of poly(lactide)/poly(butylene adipate-co-terephthalate) blend films using a solvent casting method and their food packaging application. *Lebensmittel-Wissenschaft + Technologie*, *68*, 454-461. http://dx.doi.org/10.1016/j.lwt.2015.12.062.
28. Harnnecker, F., Rosa, D. S., & Lenz, D. M. (2011). Biodegradable polyester-based blend reinforced with Curauá fiber: thermal, mechanical and biodegradation behaviour. *Journal of Polymers and the Environment*, *20*(1), 237-244. http://dx.doi.org/10.1007/s10924-011-0382-5.
29. Pujari, R. (2021). *Ageing performance of biodegradable PLA for durable applications* (Doctoral dissertation). Rochester Institute of Technology, USA.
30. Oliveira, M., Santos, E., Araújo, A., Fechine, G. J. M., Machado, A. V., & Botelho, G. (2016). The role of shear and stabilizer on PLA degradation. *Polymer Testing*, *51*, 109-116. http://dx.doi.org/10.1016/j.polymertesting.2016.03.005.
31. Wu, C.-S. (2003). Physical properties and biodegradability of maleated-polycaprolactone/starch composite. *Polymer Degradation & Stability*, *80*(1), 127-134. http://dx.doi.org/10.1016/S0141-3910(02)00393-2.
32. Phetwarotai, W., Zawong, M., Phusunti, N., & Aht-Ong, D. (2021). Toughening and thermal characteristics of plasticized polylactide and poly(butylene adipate-co-terephthalate) blend films: influence of compatibilization. *International Journal of Biological Macromolecules*, *183*, 346-357. http://dx.doi.org/10.1016/j.ijbiomac.2021.04.172. PMid:33932412.
33. Pavia, D. L., Lampman, G. M., Kriz, G. S., & Vyvyan, J. (2015). *Introdução à espectroscopia*. São Paulo: Cengage Learning.
34. Palsikowski, P. A., Kuchnier, C. N., Pinheiro, I. F., & Morales, A. R. (2017). Biodegradation in soil of PLA/PBAT blends compatibilized with chain extender. *Journal of Polymers and the Environment*, *26*(1), 330-341. http://dx.doi.org/10.1007/s10924-017-0951-3.
35. Kumar, M., Mohanty, S., Nayak, S. K., & Parvaiz, M. R. (2010). Effect of glycidyl methacrylate (GMA) on the thermal, mechanical and morphological property of biodegradable

PLA/PBAT blend and its nanocomposites. *Bioresource Technology*, *101*(21), 8406-8415. http://dx.doi.org/10.1016/j.biortech.2010.05.075. PMid:20573502.

36. Signori, F., Coltelli, M.-B., & Bronco, S. (2009). Thermal degradation of poly(lactic acid) (PLA) and poly(butylene adipate-co-terephthalate) (PBAT) and their blends upon melt processing. *Polymer Degradation & Stability*, *94*(1), 74-82. http://dx.doi.org/10.1016/j.polymdegradstab.2008.10.004.

Received: July 08, 2022
Revised: Oct. 18, 2022
Accepted: Oct. 25, 2022